ELSEVIER

Deep-Sea Research II 51 (2004) 799–816

DEEP-SEA RESEARCH
PART II

www.elsevier.com/locate/dsr2

Phytoplankton absorption, photosynthetic parameters, and primary production off Baja California: summer and autumn 1998

Elsa Aguirre-Hernández[a], Gilberto Gaxiola-Castro[a,*], Sila Nájera-Martínez[a], Timothy Baumgartner[a,b], Mati Kahru[b], B. Greg Mitchell[b]

[a]*Departamento de Oceanografía Biológica, División de Oceanología, Centro de Investigación Científica y de Educación Superior de Ensenada, Kilómetro 107 Carretera Tijuana-Ensenada, Ensenada, Baja California, México*
[b]*Scripps Institution of Oceanography, University of California, San Diego, La Jolla, CA, USA*

Received 24 February 2003; accepted 3 May 2004

Abstract

To estimate ocean primary production at large space and time scales, it is necessary to use models combined with ocean-color satellite data. Detailed estimates of primary production are typically done at only a few representative stations. To get survey-scale estimates of primary production, one must introduce routinely measured Chlorophyll-*a* (Chl-*a*) into models. For best precision, models should be based on accurate parameterizations developed from optical and photosynthesis data collected in the region of interest. To develop regional model parameterizations ^{14}C-bicarbonate was used to estimate in situ primary production and photosynthetic parameters (α^*, P^*_m, and E_k) derived from photosynthesis–irradiance (*P–E*) experiments from IMECOCAL cruises to the southern California Current during July and October 1998. The *P–E* experiments were done for samples collected from the 50% surface light depth for which we also determined particle and phytoplankton absorption coefficients (a_p, a_ϕ, and a^*_ϕ).

Physical data collected during both surveys indicated that the 1997–1998 El Niño was abating during the summer of 1998, with a subsequent transition to the typical California Current circulation and coastal upwelling conditions. Phytoplankton chl-*a* and in situ primary production were elevated at coastal stations for both surveys, with the highest values during summer. Phytoplankton specific absorption coefficients in the blue peak ($a^*_{\phi(440)}$) ranged from 0.02 to 0.11 m^2 (mg Chl-*a*)$^{-1}$ with largest values in offshore surface waters. In general a^*_ϕ was lower at depth compared to the surface. *P–E* samples were collected at the 50% light level that was usually in the surface mixed layer. Using α^* and spectral absorption, we estimated maximum photosynthetic quantum yields (ϕ_{max}; mol C/mol quanta). ϕ_{max} values were lowest in offshore surface waters, with a total range of 0.01–0.07. Mean values of ϕ_{max} for July and October were 0.011 and 0.022, respectively. In July P^*_m was approximately double and α^* was about 1.4 times the values for October. Since the *P–E* samples were generally within the upper mixed layer, these tendencies in the photosynthetic parameters are attributed to deeper mixing of this layer during October when the mean mixed layer for the photosynthesis stations

*Corresponding author. Fax: +52-646-175-0545.
E-mail address: ggaxiola@cicese.mx (G. Gaxiola-Castro).

0967-0645/$ - see front matter
doi:10.1016/j.dsr2.2004.05.015

was 35 m compared to a mean of 10 m in July. Application of a semi-analytical model using mean values of P–E parameters determined at the 50% light depth provided good agreement with ^{14}C in situ estimates at the discrete 50% light depth and for the water-column integrated primary production.

1. Introduction

Phytoplankton biomass and primary production are the foundation of the pelagic ocean ecosystem, and therefore fundamental to understanding oceanic carbon cycles, fisheries, and the coupling of pelagic ecosystems to regional-and basin-scale physical–chemical forcing. With the advent of operational ocean-color satellites it is now possible to estimate phytoplankton biomass and primary production on large spatial scales and to study the variability caused by interannual climate forcing such as El Niño (Kahru and Mitchell, 2000, 2002). Several semi-analytical models for estimating primary production incorporate phytoplankton photosynthetic parameters derived from photosynthesis–irradiance (P–E) relationships determined for natural communities (Platt et al., 1988; Sathyendranath et al., 1989; Sakshaug et al., 1997). Platt and Sathyendranath (1988) proposed a semi-analytical model of primary production that incorporates biogeographic variations in the phytoplankton response to irradiance (α^*, the coefficient of maximum light utilization, P^*_m, the rate of maximum photosynthesis, and E_k, the light saturation parameter). They recommended using mean photosynthetic parameters determined for different regions and satellite estimates of surface irradiance (PAR; μmol quanta $m^{-2} s^{-1}$) and chlorophyll-a (Chl-a), to estimate primary production from the regional to the global scale. These models are useful for estimating primary production when only Chl-a estimates are available. Ideally, model parameters should be evaluated for the oceanic domain of interest before applying them in the model.

For the southern region of the California Current off Baja California, variability in primary production and the underlying parameters required for implementing photosynthesis models have not been studied in detail. This is a region with strong interannual forcing from El Niño cycles (Kahru and Mitchell, 2002) and dynamic mesoscale responses to synoptic events including wind-driven upwelling. To understand primary production, ecosystem status, and organic carbon flux for this region, the appropriate phytoplankton optical and photosynthetic rate parameters must be specified.

From autumn 1997 to spring 1998 a major El Niño event occurred in the California Current System (Hayward et al., 1999), resulting in anomalous values of temperature and salinity in surface waters starting in October 1997 (Lynn et al., 1998; Durazo and Baumgartner, 2002). Physical and biological changes in the pelagic environment off Baja California associated with this event have been reported elsewhere (Lynn et al., 1998; Hayward et al., 1999; Bograd et al., 2000; Kahru and Mitchell, 2000; 2002; Durazo et al., 2001; Durazo and Baumgartner, 2002; Lavaniegos et al., 2002). In July and October 1998, oceanographic surveys were completed off Baja California by the IMECOCAL program (Investigaciones Mexicanas de la Corriente de California). During these two surveys, in situ primary production estimates based on radiocarbon (^{14}C) incorporation were accomplished for the first time in the southern region of the California Current. Concurrent estimates of phytoplankton P–E parameters were determined daily at the 50% irradiance depth. Using mean values of P–E parameters for each cruise, and measured profiles of Chl-a and irradiance, we applied a semi-analytical model to our full station grid to estimate primary production for the region. The model performance was evaluated by comparing with results of in situ ^{14}C-bicarbonate incubations for both discrete depth values (50% irradiance depth) and depth-integrated values.

2. Methods

During July (cruise 9807) and September–October 1998 (9810) surveys were conducted in the southern region of the California Current off Baja California, aboard *R/V Francisco de Ulloa* operated by CICESE (Centro de Investigación Científica y de Educación Superior de Ensenada). On these surveys CTD profiles and bottle casts were done at each station with a SeaBird CTD and a General Oceanics rosette with Niskin sample bottles. To minimize contamination, the Niskin bottles were configured with General Oceanic silicone tubing and o-rings (GO-81-5014, and GO-81-0012). In situ primary productivity incubations with ^{14}C-bicarbonate were performed near local noon each day. Water samples were collected in 5-l Niskin bottles from the 100, 50, 30, 20, 10, and 1% surface irradiance depths. These depths were calculated according to Beer's Law [$Z = \ln(E_o/E_z)/K_d$]; the vertical light attenuation coefficient (K_d) was estimated from the Secchi Disk depth (Z_{SD}) using the equation $K_d = 1.7/Z_{SD}$ (Parsons et al., 1984). Profiles and surface estimates of spectral downwelling irradiance, E_d (λ,z), at six wavelengths (412, 443, 490, 510, 555, and 565 nm), and $E_{PAR}(z)$ (μmol quanta $m^{-2}\,s^{-1}$) were measured with a profiling spectral radiometer (PRR-600 profiler and PRR-610 surface reference; Biospherical Instruments Inc.). During profiles the ship was oriented to minimize ship shadow artifacts.

For phytoplankton Chl-*a*, and absorption coefficients, one litre of seawater was filtered onto Whatman GF/F glass fiber filters using positive pressure. Filters were placed immediately in liquid nitrogen until post-cruise analysis. Phytoplankton Chl-*a* was extracted with 90% acetone for 24 hours in a dark refrigerator (~4 °C), following the procedure of Venrick and Hayward (1984). Pigment concentration was analyzed by the fluorometric method (Yentsch and Menzel, 1963; Holm Hansen et al., 1965), with a Turner Designs 10-AU-05 fluorometer, calibrated with pure Chl-*a* (Sigma). Total particle spectral absorption [$a_{p(\lambda)}$], and absorption of detrital particles after methanol extraction of pigments [$a_{d(\lambda)}$] were determined with a Varian Cary 1E UV-Visible spectrophotometer using standard methods (Mitchell et al., 2002). Absorption spectra were corrected for the light pathlength amplification caused by light scattering in the filter with the equations for GF/F filters recommended by Mitchell (1990). Phytoplankton absorption coefficients [$a_{\phi(\lambda)}$] were calculated as the difference between total particle and methanol extracted absorption: $a_{\phi(\lambda)} = a_{p(\lambda)} - a_{d(\lambda)}$ (Kishino et al., 1985). The Chl-*a* specific spectral absorption coefficient [$a^*_{\phi(\lambda)}$] was obtained by normalizing the phytoplankton absorption coefficients by the fluorometric Chl-*a* determined for the same sample: $a^*_{\phi(\lambda)} = a_{\phi(\lambda)})/Chl - a$; m^2 (mg Chl-*a*)$^{-1}$.

From the 100, 50, 30, 20, 10, and 1% E_o light depths, water samples were screened through a 150 μm-net to exclude macrozooplankton and inoculated with ~5 μCi $NaH^{14}CO_3$ in 250-ml polycarbonate sample bottles. To estimate the rates of in situ primary production (P; mgC $m^{-3}\,h^{-1}$), duplicate light bottles from each depth were placed into a transparent acrylic tube, together with one dark bottle for each depth, and deployed to their original sampling depth for approximately 2 h near local noon.

After incubation, samples were filtered onto 0.45-μm pore Millepore HA filters. To purge $NaH^{14}CO_3$ that was not fixed by photosynthesis, filters were placed in 20-ml scintillation vials with 0.5 ml of 10% HCl for 3 hours. Scintillation cocktail (10 ml Ecolite) was then added to each vial, and the radioactivity was determined with a Beckman LS-5000 scintillation counter. Primary production values (mg C $m^{-3}\,h^{-1}$) were calculated from these radioactivity counts, according to Parsons et al. (1984), subtracting the carbon uptake of the dark bottles.

Phytoplankton photosynthetic parameters [P^*_m, mg C (mg Chl-*a*)$^{-1}$ h^{-1}; α^*, mg C h^{-1} (mg Chl-*a*)$^{-1}$/μmol quanta $m^{-2}\,s^{-1}$ and E_k μmol quanta $m^{-2}\,s^{-1}$] were calculated from P–E experiments with water collected from the 50% irradiance depth. Aliquots of the sample were placed in 27 transparent 250-ml polystyrene phytoplankton culture flasks (Nunclon, Inc.). Five microCurie $NaH^{14}CO_3$ was added to each flask and the samples were incubated for approximately 2 h in a light gradient ranging from 5 to 500 μmol quanta $m^{-2}\,s^{-1}$. The incubator had a

500-W tungsten–halogen lamp, and the design was based on the system described by Babin et al. (1994). The intensity of light within each sample position was determined with a Biospherical Instruments, Inc. QSL-100 PAR meter. The light attenuation of this type of system is achieved by the inverse of the squared distance. We measured irradiance in the incubator using a Biospherical Instruments, Inc. MER 2041 13-channel surface irradiance sensor covering the spectral range 340–865 nm.

After incubation, *P–E* samples were filtered, acidified, and radioactivity was calculated as described above, after subtracting the time zero values. Rates of carbon uptake were normalized by the sample chlorophyll-*a* [P^*; mg C (mg Chl-*a*)$^{-1}$ h^{-1}]. Photosynthetic parameters (P^*_m and α^*) were estimated using the equation of Jassby and Platt (1976): $P^* = P^*_m \tanh\left[E_s\alpha^*)/P^*_m\right]$ where E_S is the irradiance measured inside each sample bottle, α^* and P^*_m are the coefficient of maximum light utilization, and the rate of maximum photosynthesis at light saturation, respectively. The light saturation parameter E_k is defined as the ratio P^*_m/α^*. The parameters estimated by fitting this equation to the data typically accounted for more than 90% of the variance. However, because the accurate values of P^*_m were not totally reached with the incubation and fitting procedures, we can consider these determinations as a first approximation to the measured data.

We used α^* values derived from *P* vs. *E* curves, and phytoplankton specific absorption coefficients normalized to the lamp irradiance spectrum [$\bar{a}^*_{\phi(\mathrm{PAR})}$] to calculate the maximum quantum yield of photosynthesis ($\phi_{\max}$; mol C/mol quanta) from the equation: $\phi_{\max} = \alpha^*/\bar{a}^*_{\phi(\mathrm{PAR})}$ (e.g. Cota et al., 1994; Sosik, 1996). We calculated spectrally weighted values of the phytoplankton specific absorption coefficients [$\bar{a}^*_{\phi(\mathrm{PAR})}$] for photosynthetically active radiation (PAR; 400–700 nm) in the incubator using the phytoplankton absorption spectrum of the sample, and the spectral shape of the incubation lamp determined with the 13-channel MER 1041 spectral radiometer [see Moisan and Mitchell (1999) for details].

Integrated primary production was modeled using the equations of Platt and Sathyendranath (1988) with measured profiles of Chl-*a* and regional averages of photosynthetic parameters from the 50% E_o depth. To model primary production at all stations (e.g. night and daytime stations) in the survey grid, the mean surface irradiance during daily incubations and the mean profile of PAR irradiance for daylight stations within a 24-h period were used with Chl-*a* from each station during the same day. We evaluated the performance of the Platt and Sathyendranth model with constant parameters (mean values each month of α^* and P^*_m for the 50% light depth) and a depth-dependent coefficient α^*. The depth-dependent coefficient [$\alpha^*_{(z)}$] was calculated from $\phi_{(Z)}$ and $\bar{a}^*_{\phi(z)}$ using the equation of Schofield et al. (1993). We did not consider the potential diel variations in *P–E* parameters previously reported for the California Current region (Harding et al., 1982).

Mixed layer depths for each primary production and *P-E* station were specified as the depth where the temperature was 0.5 °C less than the surface temperature, following the criteria of Tomczak and Godfrey (1994). As a proxy for the nutricline depth, the 15 °C isotherm was determined for the surveyed region using the CTD data.

3. Results

3.1. Surface chlorophyll and temperature

Hydrographic data collected during the July and October IMECOCAL surveys are described in more detail in Durazo and Baumgartner (2002). Monthly composites of satellite estimates of Chl-*a* and sea-surface temperature (SST) are shown in Fig. 1. Stations with the circle in satellite Chl-*a* maps (Figs. 1A and B) correspond to the locations of primary production experiments (see also Table 1 for details). Highest Chl-*a* values were found in coastal waters associated with colder upwelled water. The satellite SST patterns reveals general oceanographic features within the station grid that are consistent with the earlier hydrographic report. The coldest waters associated with coastal upwelling were observed in October but both cruises had coldest SST near the coast (Fig. 1C and D). The warmest waters each cruise were found in the

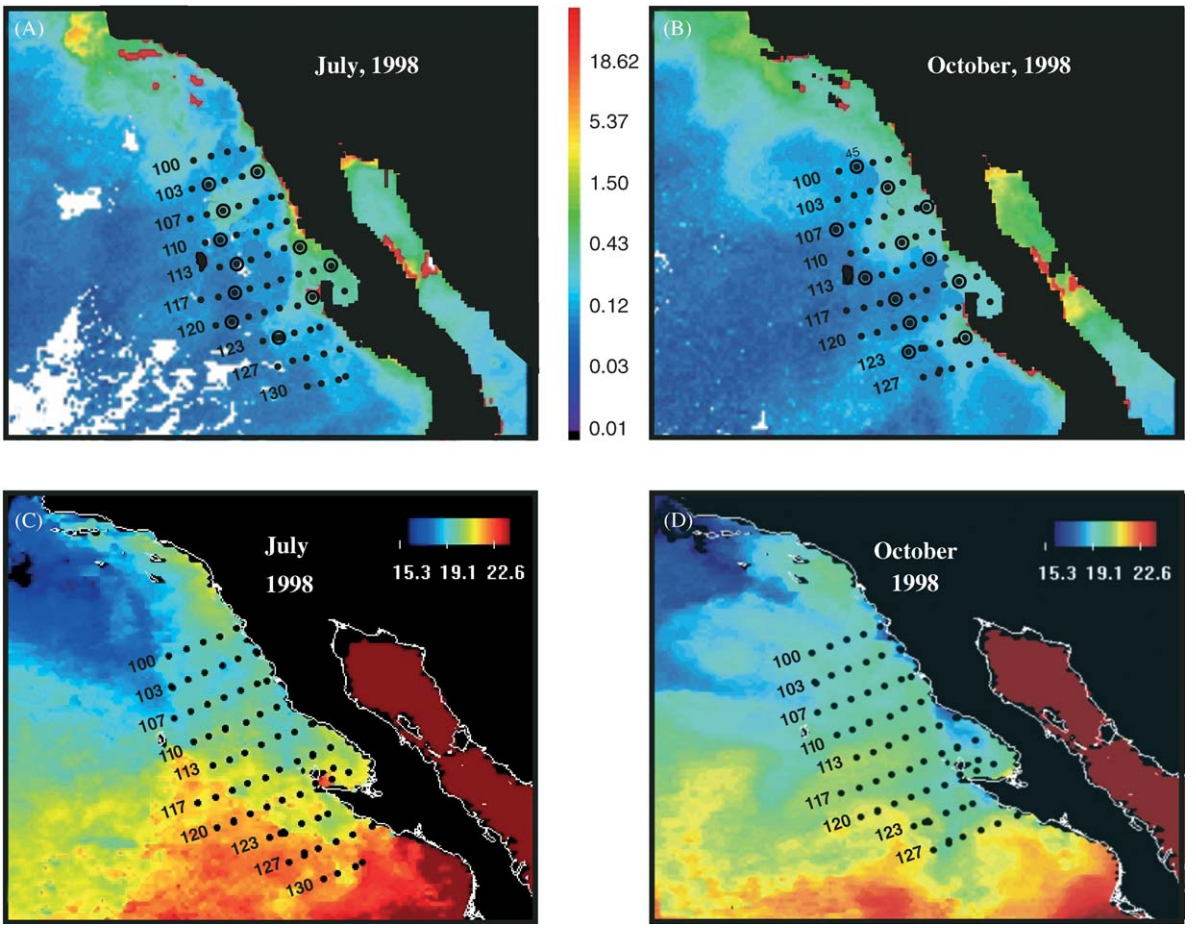

Fig. 1. SeaWiFS estimates of surface chlorophyll for high-resolution LAC composite imagery for July, 1998 (A) and October, 1998 (B). Location of stations visited during IMECOCAL surveys are indicated. The stations with open circle symbols indicate locations where in situ primary production and P vs. E incubations were done. Color scale in units of mg Chl-a m^{-3}. NOAA AVHRR sea surface temperature composites for July, 1998 (C) and October, 1998 (D). Temperature color scale in units of °C.

southwest region of the survey; both ship and satellite data had surface temperature as high as 24 °C in July (Hayward et al., 1999; Durazo and Baumgartner, 2002). A third area in the middle of the grid and toward the north had intermediate surface temperatures suggesting a mixing zone between colder waters of the CCS coming from the north, and the warmer sub-tropical waters from the southwest.

Although the coldest surface waters, associated with upwelling events, were observed at inshore locations during October, intensification of equator-ward flow as reported by Durazo and Baumgartner (2002) may have contributed to cooler SST during this month, especially in the southwest part of the grid. For both July and October considerable mesoscale variability is evident in the satellite images; station 103.30 in July was the coldest station of the two cruises where in situ photosynthesis studies were done (Table 1). For primary production stations the mean depth of the mixed layer (MLD) was 10 m (SE = 2 m) in July and 35 m (SE = 4 m) in October. Both cruises had a similar range in euphotic zone depths with Z_{EU}

Table 1
Location, depth of 50% PAR light level (Z_{PE}), temperature at the 50% E_o depth (T), mixed layer depth (MLD), integrated Chl-*a* (CHLi), integrated primary production (P), chlorophyll at 50% E_o depth ($CHL_{50\%}$), and photosynthetic parameter ($P^*_{m,}$ α^*, E_k, ϕ_{max}) at selected stations where photosynthesis process studies were done during IMECOCAL cruises in July and October, 1998.

CRUISE	STA	LAT	LONG	Z_{PE}	T (°C)[1]	MLD (m)	CHL_i (mg Chl-*a* m^{-2})	P (mg C m^{-2} h^{-1})	$CHL_{50\%}$ (mg Chl-*a* m^{-3})	P^*_m [mg C (mg Chl-*a* h)$^{-1}$]	α^* [mg C (mg Chl-*a* h)$^{-1}$ (μmol quanta m^{-2} s^{-1})$^{-1}$]	E_k (μmol quanta m^{-2} s^{-1})	φ_{max} [mole carbon (mole quanta absorbed)$^{-1}$]
9807	103.30*	31 06	116 24	7	16.2	3.4	20	55	0.42	11.26	0.028	402	Nd
	107.50	29 50	117 21	7	18.4	8.2	26	63	0.42	7.95	0.011	723	Nd
	110.50	29 15	117 00	12	18.6	7.7	20	21	0.18	Nd	0.004	Nd	0.006
	113.30*	29 22	115 17	6	18.8	19.3	21	96	0.59	7.72	0.011	702	0.015
	113.55	28 31	116 56	9	20.9	11.8	12	12	0.20	3.06	0.007	437	0.008
	117.35*	28 38	115 17	7	20.1	14.0	19	83	0.46	5.73	0.011	521	Nd
	117.60	27 47	116 52	9	21.1	7.6	15	22	0.17	3.13	0.007	447	0.013
	120.40*	27 56	115 13	7	18.0	7.9	13	50	0.70	4.14	0.011	376	Nd
	Mean	—	—	8.0	19.0	9.9	18.25	50.25	0.39	6.14	0.011	515	0.011
	Std. Error	—	—	±0.7	±0.6	±1.7	±1.64	±10.74	±0.07	±1.14	± 0.003	±54	±0.002
9810	100.45*	31 11	117 46	6	19.9	27.2	5	4	0.27	0.51	0.005	102	0.009
	103.40*	30 45	117 04	7	20.3	19.9	19	20	0.35	2.49	0.007	356	0.019
	107.35*	30 21	116 22	7	18.8	25.4	21	24	0.47	3.06	0.010	306	0.069
	107.60	29 30	118 01	13	18.6	36.3	19	14	0.20	2.26	0.007	323	Nd
	110.45	29 25	116 36	13	19.3	35.8	29	29	0.28	2.97	0.009	330	Nd
	113.40*	29 03	115 57	12	19.5	50.2	21	22	0.25	4.89	0.009	543	Nd
	113.60	28 21	117 15	12	20.2	60.0	20	24	0.28	3.38	0.009	376	0.015
	117.40*	28 27	115 35	7	19.3	19.2	27	22	0.43	3.94	0.008	493	0.019
	117.65	27 37	117 13	7	19.9	30.2	13	11	0.25	5.50	0.006	917	Nd
	120.60	27 12	116 30	12	20.5	38.1	11	19	0.29	3.52	0.007	503	0.015
	123.42*	27 14	114 58	14	20.8	32.1	18	27	0.25	2.97	0.007	424	0.011
	123.60	26 39	116 08	12	20.5	50.7	17	10	0.24	2.58	0.008	323	0.019
	Mean	—		10.2	19.8	35.4	18.33	18.83	0.30	3.17	0.008	416	0.022
	Std. Error	—		±0.9	±0.2	±3.7	±1.88	±2.18	±0.02	±0.37	±0.0004	±56	±0.007

The depth of the euphotic zone (Z_{EU}) can be estimated from Z_{PE} and the equations in methods. Nd = no data.
*Inshore stations.
[1]At 50% E_o level.

ranging from ~35 m at inshore locations to ~85 m at offshore stations. For inshore stations the deep chlorophyll maximum layer (DCM) was generally very shallow (from 15 to 25 m) and associated with a shallower thermocline. Offshore, the DCM was generally deeper than 80 m.

Contour plots of Chl-*a* concentrations at 10-m for each survey are shown in Fig. 2. During July, ship data indicated high values associated with an apparent eddy off Punta Baja (~29.5°N, 116.5°W), and at inshore areas from Punta Baja to Vizcaino Bay (~28°N, 114.5°W). Most of our study area during July had near-surface chlorophyll concentrations $<0.40\,\mathrm{mg\,Chl\text{-}a\,m^{-3}}$ (Fig. 2A), but during October the 10-m chlorophyll concentrations tended to be higher particularly at inshore locations between San Quintin Bay (~30.5°N) and Punta San Hipolito (27.0°N) (Fig. 2B). The satellite Chl-*a* in Figs. 1A and B generally agree with the ship data but have better spatial resolution compared to the low resolution of the ship survey.

There is conflicting evidence regarding the onset of equator-ward flow following the large El Niño of 1997–1998. Analysis of hydrographic cruises including CalCOFI and IMECOCAL confirmed a transition was occurring by mid-1998 (Hayward et al., 1999; Durazo and Baumgartner, 2002). Analysis of satellite sea surface temperature anomalies showed an initial return toward cooler waters in mid-summer 1998 for the IMECOCAL region, a strong reversal toward warm water in late summer and early autumn, then a very rapid transition to very cold anomalies in temperature by late 1998 (Kahru and Mitchell, 2000). Based on the monthly resolution of the satellite data, it is evident that the July cruise took place as the mid-summer cold anomaly was reversing toward warm conditions, and the October cruise occurred at the end of the brief warm reversal.

For phytoplankton, the access to nutrients is fundamental to biomass accumulation. In the southern region of the California Current, major nutrients such as nitrate are generally depleted at temperatures warmer than ~15 °C (Hernández-de-la-Torre et al., 2003). While we do not have nutrient data for these cruises, the depth of the 15 °C isotherm is a convenient proxy for the

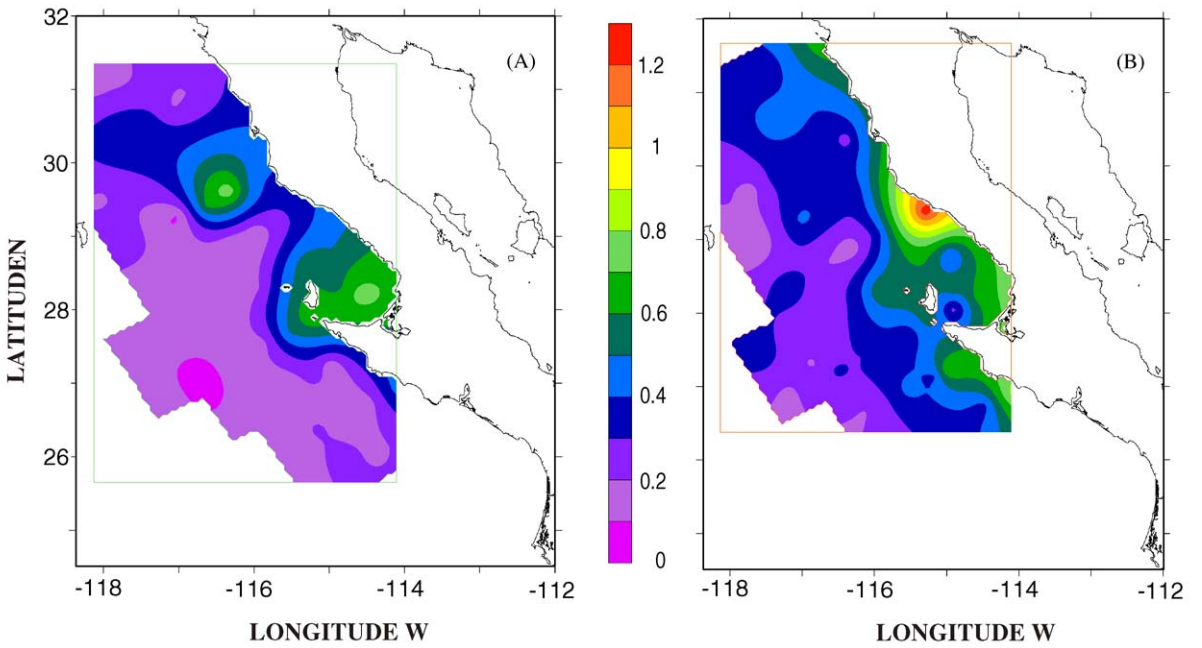

Fig. 2. Ten meter chlorophyll-*a* interpolated data from stations indicated in Fig. 1: (A) July, and (B) October 1998. Color scale indicates the Chl-*a* concentration ($\mathrm{mg\,m^{-3}}$).

relative proximity to inorganic nutrients. For the productivity stations summarized in Table 1, the mean depth of the 15 °C isotherm was 64 m (SE = 11 m) in July and 75 m (SE = 7 m) in October (Figs. 6C and D). For stations that were located inshore (asterisk in Table 1), the mean depth of this isotherm was 47 m (SE = 12 m) and 60 m (SE = 8 m) in July and October, respectively, but for offshore stations, the mean was not significantly ($p > 0.05$) different between cruises [80 m (SE = 17 m) in July; 89 m (SE = 8 m) in October].

3.2. Phytoplankton absorption

Chl-*a* specific phytoplankton absorption spectra are shown in Fig. 3. In vivo absorption of Chl-*a* creates peaks at 440 and 675 nm; various photosynthetic accessory and photoprotective pigments also absorb in the region 400–550 nm, depending on community type and their acclimation status. From 650 to 700 nm chlorophylls *a*, *b*, and *c* contribute to the absorption with the 675 nm peak of Chl-*a* dominating. Chl-*b* and *c* broaden the red peak and cause shoulders in the spectra at their respective absorption maximum. The magnitude of the absorption per unit Chl-*a* at the blue and red peaks can be interpreted with respect to photo-acclimation, ratios of photosynthetic to photoprotective pigments, detritus absorption, and pigment packaging (Morel and Bricaud, 1981; Mitchell and Kiefer, 1988a; Sosik and Mitchell, 1995; Bricaud et al., 1998; Moisan and Mitchell, 1999). Median values of a^*_ϕ m^2 (mg Chl-*a*)$^{-1}$ at 440 and 675 nm, respectively, were 0.066 and 0.0148 in July and 0.061 and 0.0153 in October. While the medians were similar between the two surveys, the highest values were observed in warm surface waters during July with stations of this type having $a^*_{\phi(440)}$ ranging from 0.08 to 0.11.

Figs. 3C and D illustrate a^*_ϕ at different light depths for example stations in the middle of the IMECOCAL grid from the two surveys. During July, a^*_ϕ tended to be higher, especially near the surface. While there was a general trend of decreasing a^*_ϕ with depth, station 113.60 in October had the lowest values at the 10% light level, with a spectrum indicating significant pigment packaging, while the 1% light level at this station had higher a^*_ϕ. We speculate that the 1% light level was dominated by picoplankton (e.g. *Synechococcus*) whose small cell size minimized the package effect, while the 10% light level may have had larger cells, for example diatoms, with more severe influence of pigment packaging and hence lower Chl-*a* specific absorption. Because we use the Mitchell (1990) β-correction for absorption coefficients calculations, which is 30% higher that the determined by *Synechococcus* (Moore et al., 1995), this could have an effect on our estimations of $a^*_{\phi(440)}$ when this picoplankton group is dominant. Higher values of $a^*_{\phi(440)}$ associated with picoplankton cells abundance has been reported for the same region by Millán-Nuñez et al. (2004) during winter 2001, with lower values of $a^*_{\phi(440)}$ when diatoms were the dominant phytoplankton group.

From both surveys, absorption spectra often had shoulders between 470 and 490 nm (Fig. 3) caused by various carotenoid accessory pigments. In October more pronounced absorption spectra shoulders near 470–480 nm were observed (Fig. 3D), with some of the most significant shoulders found at the 1% E_o level. These absorption characteristics may be caused by zeaxanthin, a characteristic pigment of *Synechococcus*. Detailed analysis of pigments by HPLC would be required to confirm our hypothesis. Surface values of a^*_ϕ were lower in October than in July. Low values of $a^*_{\phi(440)}$ in coastal waters, and also slightly lower median values for October, might be associated with better nutrient conditions for phytoplankton (e.g. shallower depth of the 15 °C isotherm). For a fixed light level, higher nutrient flux led to decreased cellular concentrations of photoprotective pigments and increased concentrations of photosynthetic pigments in nutrient-limited chemostat cultures (Sosik and Mitchell, 1994). Also, higher nutrient regimes generally tend to have a greater proportion of large phytoplankton whose cellular optics will lead to lower Chl-*a* specific absorption caused by stronger pigment package effects (Morel and Bricaud, 1981; Mitchell and Kiefer, 1988b).

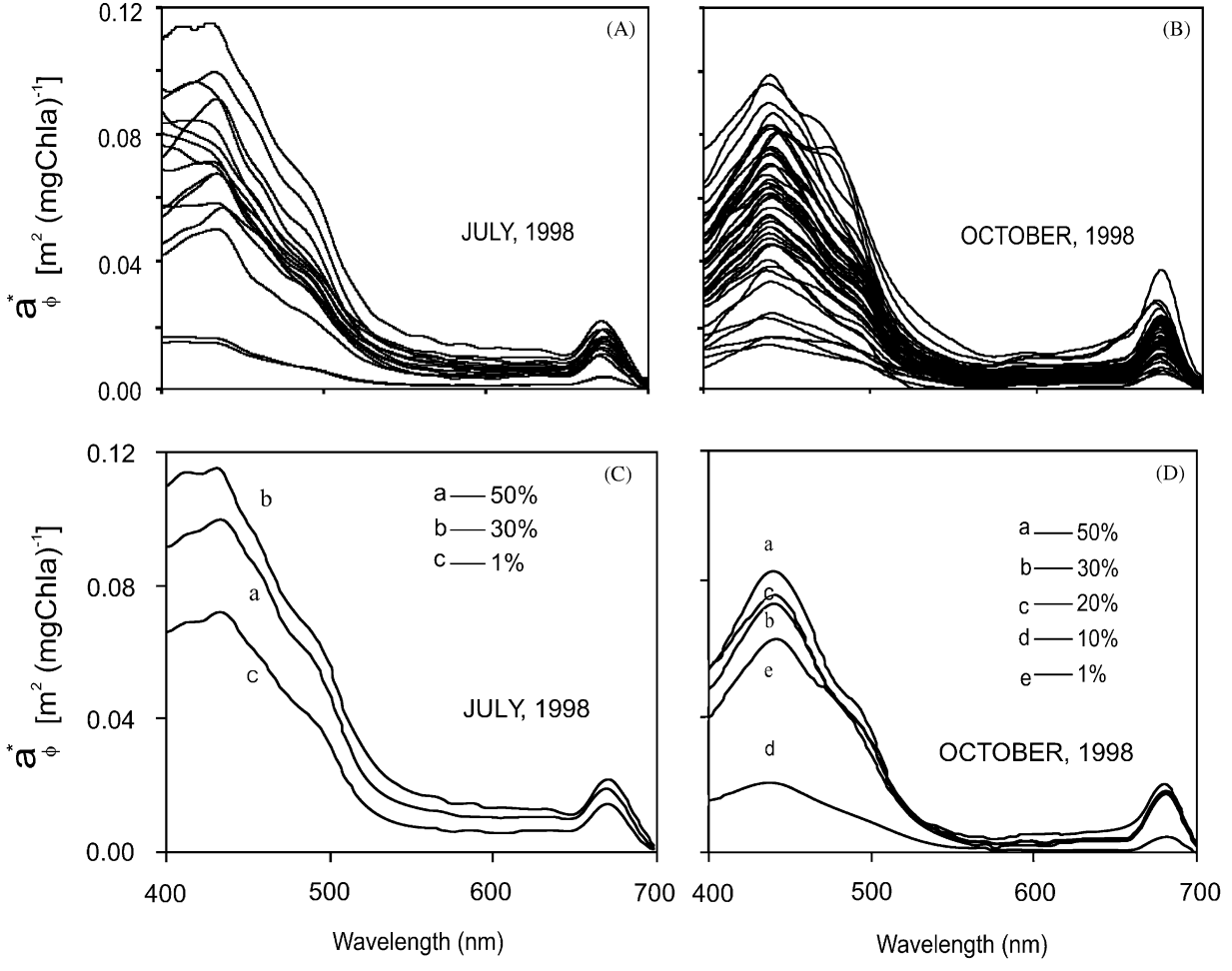

Fig. 3. Phytoplankton specific absorption spectra for all samples collected at primary production locations illustrated in Fig. 1 for July, (A) and October (B). Examples of the a^*_ϕ spectra at different depths for station 113.55 in July (C) and station 113.60 in October (D).

3.3. Primary production

Primary production estimates based on in situ ^{14}C incubations and the station coordinates are summarized in Table 1. Note these production rates are not scaled to the amount of incident irradiance so some of the variability is expected to be from variations in surface light. In July, inshore stations had higher production rates (~7.0 mg $C\,m^{-3}\,h^{-1}$), with integrated production rates for inshore stations as high as 96 mg $C\,m^{-2}\,h^{-1}$ (station 113.30; Table 1). There is a north–south primary production gradient with stations in the southwest having rates 2–3-times lower than stations in the northeast part of the grid, which is generally consistent with the gradient in surface Chl-*a* (Table 1; Figs. 1 and 2). Lowest integrated primary production values at stations in the southwest region ranged from 12 to 25 mg $C\,m^{-2}\,h^{-1}$. Primary production in October was generally at least 2–times less than in July for both inshore and offshore locations with similar integrated Chl-*a* values (Table 1). Coastal stations in October had an average of 24 mg $C\,m^{-2}\,h^{-1}$. Interestingly, the lowest production measured, 4 mg $C\,m^{-2}\,h^{-1}$, was observed in October at a northern 'inshore' station (100.45). Satellite data indicated that this station was within a warm, low Chl-*a* water mass advected from the southwest toward the Southern California Bight (Figs. 1B and D). Offshore primary production in October ranged from 10 to 24 mg $C\,m^{-2}\,h^{-1}$, with an average of 16 mg $C\,m^{-2}\,h^{-1}$. High values of integrated production in October (>60 mg $C\,m^{-2}\,h^{-1}$) were also observed near Vizcaino Bay, a shallow and plankton-rich coastal zone.

3.4. Photosynthetic parameters

Table 1 summarizes the phytoplankton maximum light utilization parameter, maximum photosynthesis at light saturation, and light saturation parameter (α^*, P^*_m, E_k) derived from *P–E* experiments (Fig. 4) conducted with samples from the 50% E_o depth. P^*_m (mg C(mg Chl-*a*)$^{-1}$ h^{-1}) in July ranged from 3 to 11 with a regional average of ~6.0. P^*_m was highest for inshore locations, lowest values occurred at offshore stations in the southwest portion of the grid where water temperatures were warmest (Table 1). During October P^*_m ranged from 0.5 to 5; the October mean of 3.2 (SE = 0.4) was significantly lower than the July mean of 6.14 (SE = 1.1) ($p < 0.05$). Station 100.45 in October had the lowest P^*_m

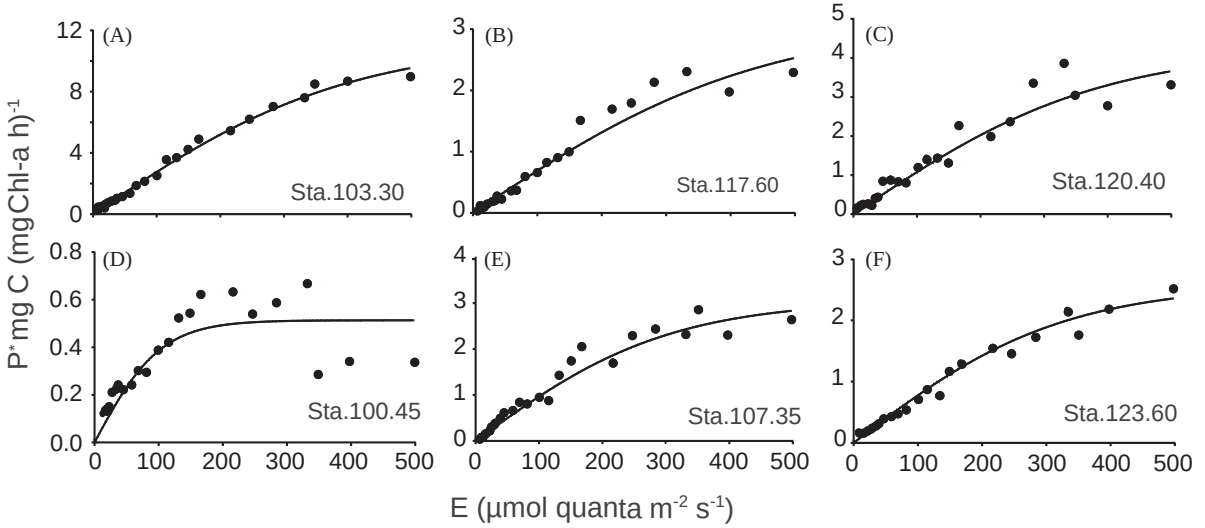

Fig. 4. Examples of *P–E* curves for representative stations from the July and October, 1998 surveys. The line shows the best fit using the Jassby and Platt (1976) equation. Note station 100.45 (D) shows evidence of photoinhibition but this was found for very few stations. Therefore, for consistency, all data were fit with no photoinhibition.

(Table 1), perhaps associated with warm, low-nutrient, surface water and a relatively deep mixed layer. The *P–E* curve in Fig. 4D indicates that this station had photoinhibition whereas most stations did not (note all were fit the same way with no photoinhibition). The susceptibility to photoinhibition also may be related to nutrient stress, low light acclimation, or both. The mean value of surface irradiance was also lower in October compared to July, which also may contribute to low light acclimation in the deeper mixed layers found during October.

Values of α^*, ranged from 0.004 to 0.028 with a mean of 0.011 (SE = 0.003) in July and from 0.005 to 0.010 with a mean of 0.008 (SE = 0.0004) in October. E_k had an overall average of 515 μmol quanta $m^{-2} s^{-1}$ for July and 416 μmol quanta $m^{-2} s^{-1}$ for October, with the lowest value for station 100.45 during October (Table 1). Estimates of the maximum quantum yield (ϕ_{max}; mol C/mol quanta) had a mean in July of 0.011 (SE = 0.002) with a range from 0.006 to 0.015. The mean was 2-times greater in October (0.022; SE = 0.007) but that result was dominated by one very high value (0.069) at station 107.35. Although the mean ϕ_{max} for July is lower than October, the opposite trend is found for mean values of α^*. We do not think this apparent discrepancy with higher ϕ_{max} but lower α^* in October compared to July is significant because we were only able to accomplish absorption and ϕ_{max} estimates at four stations in July. Three of these four stations were in low-chlorophyll waters that likely also had low nutrients and high light, both of which will lead to low quantum yields. Thus, we do not believe that our mean values for ϕ_{max} in July are representative of the full grid; there were twice as many stations where we computed α^* in July, so this parameter may be more representative.

3.5. Modeled primary production

Integrated primary production using the Platt and Sathyendranath (1988) algorithm agreed well with the ^{14}C in situ estimates but the comparison between the model and the 50% surface irradiance depth did not agree as well (Fig. 5). When the *P–E* parameters were introduced to the model with in situ estimates of Chl-*a* and PAR, the model regression compared to in situ ^{14}C estimates had a slope of 1.43 for the discrete values from the 50% E_o depth ($r = 0.92$), and a slope of 1.02 for the euphotic zone integrated values ($r = 0.83$) (Figs. 5A and B). We suspect that our irradiance model may overestimate the light at the 50% depth leading to the overestimate for the discrete depth, but that this effect is not as severe when integrated over the full water column.

We also explored the estimates of primary production allowing α^* to vary with depth by

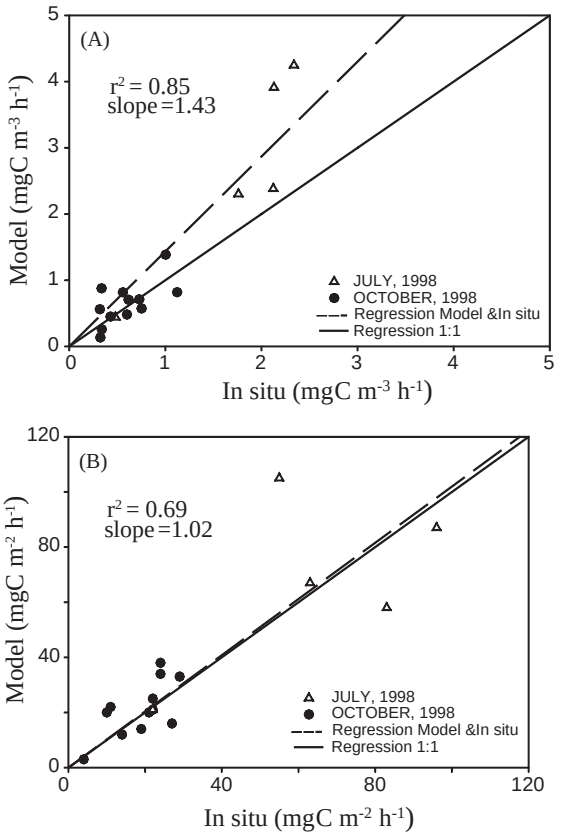

Fig. 5. (A) Relationship between discrete depth values of in situ and modeled primary production for 50% E_o depth samples. Standard deviations of the duplicate estimates for each in situ sample were always less than 0.08 mg C $m^{-3} h^{-1}$. (B) Relationship between euphotic zone (1%E_o depth) integrated primary production for in situ and modeled data. *P–E* parameters determined for the 50% E_o level were used in the depth-integrated model.

introducing our calculated values of $\phi(z)$ and $\bar{a}^*_{\phi(z)}$ into the equation of Schofield et al. (1993). This model increases α^* up to 2-times at the 10% E_o level compared to values determined by incubations of the 50% E_o sample. However, introducing this depth (light) dependence into the regional model did not significantly improve estimates of integrated primary production because modeled variability in α^* is at low light near the bottom of the euphotic zone, which contributes relatively little to the total integrated primary production.

4. Discussion

The data presented here correspond to the transition period following the strong El Niño of 1997–1998. Kahru and Mitchell (2000) showed that satellite sea–surface temperatures off Baja California from August 1997 to April 1998 were the highest in more than 20 years. By July 1998, both coastal and offshore waters had partially returned to more typical conditions. During 1999 the region was dominated by strong upwelling and anomalously cold water of La Niña. IMECOCAL survey data confirm that the region had anomalous warm waters from October 1997 to April 1998 (Durazo and Baumgartner, 2002). For July and October 1998, coastal waters were cool but not as cold as 1999, and offshore waters were still relatively warm.

The depth of the 15 °C isotherm (Figs. 6C and D) indicates that during July there were large portions of the IMECOCAL grid, particularly in the south and west, that had relatively shallow nutriclines compared to October. In the central part of the grid, very deep nutriclines were found in October, even near the coast, with a large intrusion of water with the 15 °C isotherm deeper than 100 m (Fig. 6D). Satellite data analysis indicates that the October survey may have occurred during or at the end of a short reversal toward El Niño-type conditions. Relatively warm and deep mixed layers at the productivity stations in October (Table 1), and the deeper depth of the 15 °C isotherm (Fig. 6) support this hypothesis. The satellite analysis of Kahru and Mitchell (2000) indicated that the region north of Punta Eugenia remained warm (relative to the long-term seasonal trend) late into 1998, but the region between Punta Eugenia and the tip of Baja California was in the midst of a strong transition from warm to cold sea surface temperatures during autumn 1998.

During the October survey, surface water temperatures at inshore locations were ~1.0 °C lower than corresponding summer values (Figs. 1C and D), perhaps related to the relaxation of the El Niño event (Hayward et al., 1999). While there is a general trend of cooler surface waters in October, temperatures at the 50% E_o PAR depth (Z_{PE}) sampled for P–E studies were slightly warmer (~0.8 °C on average), compared to July (Table 1), but this differences was not significant ($p<0.05$). The deeper depth of the 15 °C isotherm in October and the deep warm mixed layers for the productivity stations summarized in Table 1 are indicative of lingering El Niño conditions.

The mean value of integrated chlorophyll for our productivity stations was slightly larger in October than in July (Table 1), but the difference was not statistically significant ($p<0.05$). However, considering all the stations, inshore locations during the October survey had greater integrated Chl-a (Lavaniegos et al., 2002), possibly associated with an autumn upwelling previously reported for Baja California coastal waters (Espinosa-Carreon et al., 2001). The full hydrographic analysis of all stations in the October survey indicated both a return to more normal southward flowing cool water in the CCS and also the onset of cold coastal upwelling (Durazo and Baumgartner, 2002), both of which could augment nutrients for phytoplankton growth. However, our analysis, and the satellite results of Kahru and Mitchell (2002) suggest that October may have been in the transition from a late summer recurrence of El Niño-type conditions, especially in the southwest region, and that the general oceanographic state was perhaps mixed as the system was in the midst of rapid evolution from the late-summer warm anomaly to the late-winter very cold anomaly. Clearly, strong meso-scale structure is evident in the region during both the July and October surveys making it more difficult to use simple categories of El Niño or La Niña to characterize the grid. The infrequent ship surveys with their

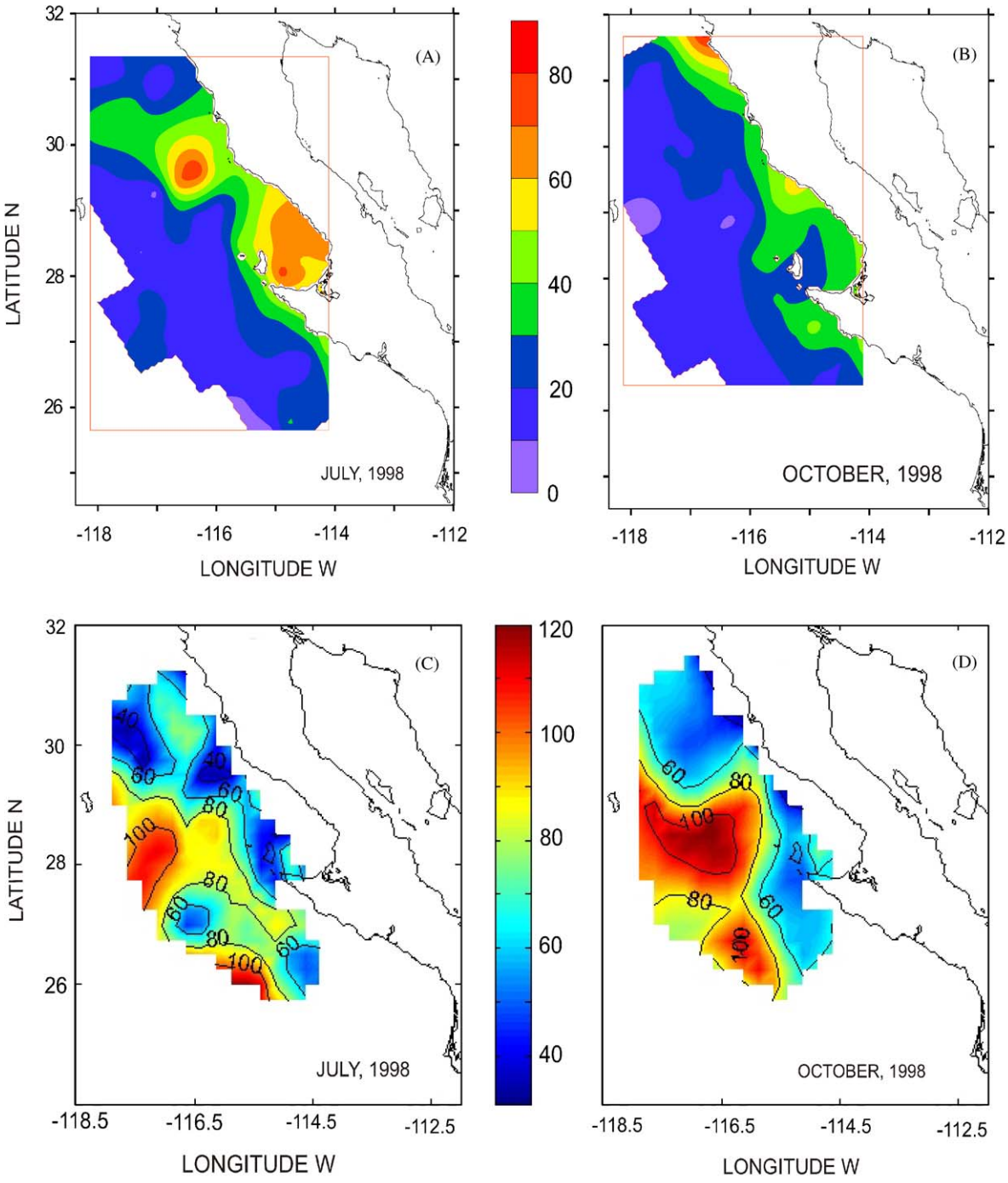

Fig. 6. Estimated water column primary production from surface to 150 m depth, using the Platt and Sathyendranath (1988) algorithm, measured Chl-*a* and PAR data. Mean *P–E* parameters for July and October were used in the model. (A) July 1998; (B) October 1998. The color scale is in units of mg C m^{-2} h^{-1}. Depth of the 15 °C isotherm during July 1998 (C) and October 1998 (D) IMECOCAL surveys. The color scale for the 15 °C isotherm is in units of meters.

relatively low spatial resolution must be interpreted together with satellite data to obtain a good synoptic perspective of the system structure.

During July, specific absorption coefficients (a^*_ϕ) were much lower inshore compared to offshore, with values of $a^*_{\phi(440)}$ as low as $\sim$0.05 m^2(mg Chl-a)$^{-1}$ in coastal waters with high Chl-*a*. This decline in $a^*_{\phi(440)}$ at higher Chl-*a* concentrations is a general phenomenon in the northeast Pacific (Mitchell and Kiefer, 1998b; Sosik and Mitchell, 1995) and elsewhere (Bricaud et al., 1995; 1998). The trend is related to a tendency toward smaller cells when Chl-*a* biomass is low, with lower intracellular concentrations of pigments, and a greater proportion of photoprotective pigments in stratified, high light, nutrient-limited regions (Mitchell and Kiefer, 1988a; Sosik and Mitchell, 1995; Nelson et al., 1993; Bricaud et al., 1995; Cleveland, 1995). High values of (a^*_ϕ) for samples collected inshore at the bottom of the euphotic zone are hypothesized to be caused by *Synechococcus* picoplankton based on their spectral shoulders at $\sim$470 nm. During the fall survey, $a^*_{\phi(440)}$ had a smaller range in surface values, but still had strong vertical variability. In general the higher values offshore are consistent with the observation that the Chl-*a* specific absorption tends to be higher in warm surface waters and for samples that are well above the depth of the nutricline (Sosik and Mitchell, 1995).

For both surveys, highest values of α^* and P^*_m were at station 103.30 in July, and the lowest were at station 100.45 in October. For 103.30 in July, the *P–E* parameters were nearly 2-times greater than the overall mean value for the July survey; this station had the coldest temperature at the 50% Eo sampling depth (Table 1). By contrast, P^*_m at station 100.45 in October was 10-times smaller than the maximum value in October, and the α^* was about 30% lower than the mean value for the October survey. Station 100.45 was in relatively warm water with very low integrated Chl-*a* (Table 1), but still had a relatively deep mixed layer of 27.2 m. Fig. 1B indicates that this station was within a warm, low Chl-*a* eddy that apparently was a water mass transported from the warm subtropical region in the southwest. The presence of these eddies has been reported by Soto-Mardones et al. (2004) off San Quintin and Punta Baja locations (30–32°N; 116–117°W). Relatively deep and warm mixed layers are typical of El Niño conditions. Fig. 6D indicates a relatively shallow depth of the 15 °C isotherm for station 100.45, indicating a possible doming of the pycnocline, and the nutricline, caused by eddy rotation. Thus warm waters from the southwest may overlay cooler nutrient-rich waters. The extremes in *P–E* parameters represented by these two stations are likely caused by differences in phytoplankton community type and environmental regulation of photosynthetic physiology (e.g. light, temperature, and nutrients). In July, P^*_m averaged 7.4 for stations with temperatures at Z_{PE} of 18 °C or less compared to an average of 5.5 for those stations with temperature greater than 18 °C at Z_{PE}. This may be related to relatively greater nutrient flux at the colder stations. The strong gradients (vertically and horizontally) observed within the IMECOCAL survey grid raise questions about the efficacy of using mean parameters for production models within regions characterized by significant mesoscale structure in temperature and nutrients.

The mean values of α^* and P^*_m in October were about half those found in July. During October, α^* also had a smaller total range compared to July (Table 1). In October, the mean value of temperature at Z_{PE} was slightly, but not significantly higher ($p > 0.05$) but mixed layer depths were significantly deeper ($p < 0.01$). Both lower P^*_m and α^* during October might be related to the significantly different mean depth of mixing during the two surveys. While the temperatures at Z_{PE} were similar in the two cruises, the MLD was very different. In general the 50% surface light levels will be saturating for most phytoplankton communities. In October Z_{PE} was always in the deeper mixed layers. Thus, we attribute the large difference in photosynthesis parameters between the surveys to low-light acclimation within deeper mixed layers during October since these populations would be acclimated to the mixing regime that would transport them below the 50% E_o level.

Acclimation of photosynthetic parameters of different taxa to a matrix of environmental control including light, nutrients and temperature are not well specified. Low light, in general, will lead to

smaller Carbon:Chl-*a* ratios that might in part lead to lower values of Chl-*a* specific carbon fixation parameters (MacIntyre et al., 2002; Geider et al., 1998). However, it is also known that nutrient and temperature regulation can lead to significant changes in the maximum quantum yield, the ratio of photosynthetic to photoprotective pigments and a^*_ϕ (Sosik and Mitchell, 1991, 1994; Moisan and Mitchell, 1999). While these general trends reported for cultures are expected to hold for diverse taxa, the individual response of different taxonomic groups may differ considerably. For example, the very high values for *P–E* parameters at station 103.30 might be caused by a combination of high light and favorable nutrients in the coldest water where we sampled for our photosynthesis studies. Thus, it is difficult to fully interpret the variations we report, especially since nutrient data and information on the composition of the phytoplankton assemblage are not available.

By introducing the measured Chl-*a*, light profiles and *P–E* parameters for the 50% light level into the model of Platt and Sathyendranath (1988) a high linear correlation coefficient was calculated ($r = 0.83$) between the integrated water column primary production and the in situ experiments (Fig. 5B). Integrated primary production (*P*) was highest for inshore stations for both cruises (Figs. 6A and B). The highest values overall were found during July. This appeared to be attributed primarily to the higher values of photosynthesis parameters in July, possibly caused by deeper mixing in and lower surface irradiance in October. Lowest values of *P* tended to be located in the southwest region. The transport of warm offshore waters by secondary eddy circulation may explain why low values of *P* (4 mg $C\,m^{-2}\,h^{-1}$) and *P–E* parameters were found near the coast at station 100.45 in October. Low primary production and surface pigment concentrations attributed to the transport of offshore water close to the coast have been reported for this region of the California Current during summer conditions (Gaxiola-Castro and Alvarez-Borrego, 1991; Peláez and McGowan, 1986).

For various applications, including fisheries management, and a general understanding of carbon cycle dynamics, it is essential to get regional estimates of integrated primary production. Ultimately, our goal will be to achieve this using only satellite data. However, significant gaps in models persist, including accurate depth resolution of the Chl-*a* biomass and the photophysiology parameters of the models as they vary in space and time. We have taken an intermediate step that combined regional estimates of mean values of *P–E* parameters for two cruises, and applied these with a depth-integrated model (Platt and Sathyendranath, 1988) to create a survey-scale map of integrated primary production for all IMECOCAL stations occupied during the July and October surveys in 1998. By combining our measured Chl-*a* and light profiles with the model, we were able to extend the limited number of photosynthesis process stations to create a near-synoptic map of integrated primary production for the region studied.

5. Conclusion

The extremes discussed above for stations 103.30 in July and 100.45 in October demonstrate that it will be important to have a robust approach to estimate dramatic changes in photosynthetic physiology that are evident within major biogeographic domains and that also will occur within a depth profile at a single station. It is important to note that these two stations are less than 100 km apart, but clearly they represent significant differences between community photophysiolgy with important implications for accurate modeling of photosynthesis. We explored using a depth-dependent α^* based on the light-dependent model of Schofield et al. (1993). This did not improve the model's skill for estimates of *P* compared to using mean values of α^* each cruise. Since we measured *P–E* relationships only at one depth, we are not able to properly scale the depth (light) dependence of α^*, although we do expect it to increase with depth as previously reported for this region (Hood et al., 1991; Schofield et al., 1993; Sosik, 1996). One reason why allowing α^* to vary with depth (light) did not improve the model skill is that the majority of the primary production occurs in the

upper part of the photic zone where variations in α^* are not relevant since the cells are photosynthesizing at P_m^* (Beherenfeld and Falkowski, 1997).

It is not yet possible to have a full understanding of the photosynthetic physiology and the most accurate parameters to model photosynthesis at each depth. The photosynthetic parameters are dependent both on the species present and their acclimation to environmental variables (light, nutrients and temperature). More detailed studies of the phytoplankton community composition and how they acclimate to physical–chemical forcing are required to improve our ability to estimate photosynthesis model parameters. We find that the variability within this small region is large. Our data suggest that the meso-scale structure across complex upwelling zones is as significant as seasonal or interannual forcing in determining the magnitudes of photosynthesis parameters required for modeling primary production. For regions such as IMECOCAL we believe it will be essential to use the meso-scale information available from satellites to specify more accurately the photosynthesis model parameters associated with the phytoplankton community and its recent acclimation history.

Acknowledgements

CICESE and CONACYT support the cruises and laboratory work under projects G0041-T9607, DAJJ002/750/00, and G-35326 T. We thank to the Captain and crew of the CICESE *R/V Francisco de Ulloa*, and all the participants in the IMECOCAL surveys. The first author had fellowships from CONACYT and from G0041-T9607 project. SeaWIFS data provided by Orbimage via the SeaWIFS project and NASA-GSFC-DAAC. NASA's Ocean Biology and SIMBIOS programs supported B.G.M. We thank to Dr. Helmut Maske and an anonymous reviewer for their comments that were very helpful. J.M. Dominguez, F. Ponce, and J. Cepeda draw final figures. This is a contribution from the IMECOCAL research program to the scientific agenda of the Eastern Pacific Consortium (EPCOR) of the Interamerican Institute for Global Change Research (IAI).

References

Babin, M., Morel, A., Gagnon, R., 1994. An incubator designed for extensive and sensitive measurements of phytoplankton photosynthetic parameters. Limnology and Oceanography 39, 694–702.

Beherenfeld, M.J., Falkowski, P.G., 1997. Photosynthetic rates derived from satellite-based chlorophyll concentration. Limnology and Oceanography 42, 1–20.

Bograd, S.J., DiGiacomo, P.M., Durazo, R., Hayward, T.L., Hyrenbach, K.D., Lynn, R.J., Mantyla, A.W., Schwing, F.B., Sydeman, W.J., Baumgartner, T., Lavaniegos, B., Moore, C.S., 2000. The State of the California Current, 1999–2000: forward to a new regime? California Cooperative Oceanic Fisheries Investigations Reports 41, 26–52.

Bricaud, A., Babin, M., Morel, A., Claustre, H., 1995. Variability in the chlorophyll-specific absorption coefficients of natural phytoplankton: analysis and parameterization. Journal of Geophysical Research 100, 13321–13332.

Bricaud, A., Morel, A., Babin, M., Allali, K., Claustre, H., 1998. Variations of light absorption by suspended particles with chlorophyll *a* concentration in oceanic (case 1) waters: analysis and implications for bio-optical models. Journal of Geophysical Research 103, 31033–31044.

Cleveland, J.S., 1995. Regional models for phytoplankton absorption as a function of chlorophyll a concentration. Journal of Geosphysical Research 100, 13333–13344.

Cota, G.F., Smith Jr., W.O., Mitchell, B.G., 1994. Photosynthesis of *Phaeocystis* in the Greenland Sea. Limnology and Oceanography 39, 948–953.

Durazo, R., Baumgartner, T.R., 2002. Evolution of oceanographic conditions off Baja California 1997–1999. Progress in Oceanography 54, 7–31.

Durazo, R., Baumgartner, T.R., Bograd, S.J., Collins, C.A., de la Campa, S., Garcia, J., Gaxiola-Castro, G., Huyer, A., Hyrenbach, K.D., Loya, D., Lynn, R.J., Schwing, F.B., Smith, R.L., Sydeman, W.J., Wheeler, P., 2001. The State of the California Current, 2000–2001: a third straight La Niña year. California Cooperative Oceanic Fisheries Investigations Reports 42, 29–60.

Espinosa-Carreon, T.L., Gaxiola-Castro, G., Robles-Pacheco, J.M., Najera-Martinez, S., 2001. Temperature, salinity, nutrients and chlorophyll a in coastal waters of the Southern California Bight. Ciencias Marinas 27, 397–422.

Gaxiola-Castro, G., Alvarez-Borrego, S., 1991. Relative assimilation numbers of phytoplankton across a seasonally recurring front in the California Current off Ensenada. California Cooperative Fisheries Investigations Reports 32, 91–96.

Geider, R.J., MacIntyre, H.L., Kana, T.M., 1998. A dynamic regulatory model of phytoplanktonic acclimation to light, nutrients, and temperature. Limnology and Oceanography 43, 679–694.

Harding Jr., L.W., Prézelin, B.B., Sweeney, B.M., Cox, J.L., 1982. Diel oscillations of the photosynthesis–irradiance (*P–I*) relationship in natural assemblages of phytoplankton. Marine Biology 67, 167–178.

Hayward, L.T., Baumgartner, T.R., Checkley, D.M., Durazo, R., Gaxiola-Castro, G., Hyrenbach, K.D., Mantyla, A.W., Mullin, M.M., Murphree, T., Schwing, F.B., Smith, P.E., Tegner, M.J., 1999. The state of the California Current in 1998–1999: transition to cool-water conditions. California Cooperative Oceanic Fisheries Investigations Reports 40, 29–62.

Hernández-de-la-Torre, B., Gaxiola-Castro, G., Alvarez-Borrego, S., Gómez-Valdes, J., Nájera-Martínez, S., 2003. Interannual variability of new production in the southern region of the California Current. Deep-Sea Research II 50, 2423–2430.

Holm Hansen, O., Lorenzen, C., Holmes, R., Strickland, J., 1965. Fluorometric determination of chlorophyll. Journal Conseil Permanent International Exploration de la Mer 30, 3–15.

Hood, R.R., Abbot, M.R., Huyer, A., 1991. Phytoplankton and photosynthetic light response in the coastal transition zone off northern California in June 1987. Journal of Geophysical Research 96, 147–169.

Jassby, D.A., Platt, T., 1976. Mathematical formulation of the relationship between photosynthesis and light for phytoplankton. Limnology and Oceanography 21, 540–547.

Kahru, M., Mitchell, B.G., 2000. Influence of the 1997–98 El Niño on the surface chlorophyll in the California Current. Geophysical Research Letters 27, 2937–2940.

Kahru, M., Mitchell, B.G., 2002. Influence of the El Niño–La Niña cycle on satellite-derived primary production in the California Current. Geophysical Research Letters 29 27-1–27-4.

Kishino, M., Takahashi, M., Okami, N., Ichimura, S., 1985. Estimation of the spectral absorption coefficients of phytoplankton in the sea. Bulletin of Marine Science 37, 634–642.

Lavaniegos, B.E., Jimenez-Perez, L.C., Gaxiola-Castro, G., 2002. Plankton response to El Niño 1997–1998 and La Niña 1999 in the southern region of the California Current. Progress in Oceanography 54, 33–58.

Lynn, R.J., Baumgartner, T., García, J., Collins, C.A., Hayward, T.L., Hyrenbach, K.D., Mantyla, A.W., Murphree, T., Shankle, A., Schwing, F.B., Sakuma, K.M., Tegner, M.J., 1998. The state of the California Current, 1997–1998, transition to El Niño conditions. California Cooperative Oceanic Fisheries Investigations Reports 39, 25–50.

MacIntyre, H.L., Kana, T.M., Anning, J., Geider, R.J., 2002. Photoacclimation of photosynthesis irradiance response curves and photosynthetic pigments in microalgae and cyanobacteria. Journal of Phycology 38, 17–38.

Millán-Nuñez, E., Sieracki, M. E., Millán-Nuñez, R., Lara-Lara, J.R., Gaxiola-Castro, G., Trees, C.C., 2004. Specific absorption coefficient and phytoplankton biomass in the southern region of the California Current. Deep-Sea Research II, this issue [doi:10.1016/j.dsr2.2004.05.023].

Mitchell, B.G., 1990. Algorithms for determining the absorption coefficient of aquatic particulates using the quantitative filter technique (QFT). SPIE Oceans Optics X 1302, 137–148.

Mitchell, B.G., Kiefer, D.A., 1988a. Chlorophyll a specific absorption and fluorescence excitation spectra for light-limited phytoplankton. Deep-Sea Research 35A, 639–663.

Mitchell, B.G., Kiefer, D.A., 1988b. Variability in pigment specific particulate fluorescence and absorption spectra in the northeastern Pacific Ocean. Deep-Sea Research 35A, 665–689.

Mitchell, B.G., Kahru, M., Wieland, J., Stramska, M., 2002. Determination of spectral absorption coefficients of particles, dissolved material and phytoplankton from discrete samples. In: Fargion, G.S., Muller, J.L. (Eds.), Ocean Optic Protocols for Satellite Ocean Color Sensor Validation, Revision 3, vol. 2. NASA Technical Memorandum 2002-210004/Rev 3-Vol 2. pp. 231–257 (Chapter 15).

Moisan, T.A., Mitchell, B.G., 1999. Photophysiological acclimation of *Phaeocystis antarctica* Karsten under light limitation. Limnology and Oceanography 44, 247–258.

Moore, L.R., Goericke, R., Chisholm, S.W., 1995. Comparative physiology of *Synechococcus* and *Prochlorococcus*: influence of light and temperature on growth, pigments, fluorescence and absorptive properties. Marine Ecology Progress Series 116, 259–275.

Morel, A., Bricaud, A., 1981. Theoretical results concerning light absorption in a discrete medium, and applications to specific absorption of phytoplankton. Deep-Sea Research 28A, 1375–1393.

Nelson, N.B., Prezelin, B.B., Bidigare, R.R., 1993. Phytoplankton light absorption and package effect in California coastal waters. Marine Ecology Progress Series 94, 217–227.

Parsons, T.R., Maita, Y., Lalli, C.M., 1984. A Manual of Chemical and Biological Methods for Seawater Analysis. Pergamon Press, Oxford, 173pp.

Pelaez, J., McGowan, J.A., 1986. Phytoplankton pigment patterns in the California Current as determined by satellite. Limnology and Oceanography 31, 927–950.

Platt, T., Sathyendranath, S., 1988. Oceanic primary production: estimation by remote sensing at local and regional scales. Science 241, 1613–1620.

Platt, T., Sathyendranath, S., Caverhill, C.M., Lewis, M.R., 1988. Ocean primary production and available light: further algorithms for remote sensing. Deep-Sea Research 35A, 855–879.

Sakshaug, E., Bricaud, A., Dandonneau, Y., Falkowski, P.G., Kiefer, D.A., Legendre, L., Morel, A., Parslow, J., Takahashi, M., 1997. Parameters of photosynthesis: definitions, theory and interpretation of results. Journal of Plankton Research 19, 1637–1670.

Sathyendranath, S., Platt, T., Caverhill, C.M., Warnock, R.E., Lewis, M.R., 1989. Remote sensing of oceanic production: computation using a spectral model. Deep-Sea Research 36A, 431–453.

Schofield, O., Prézelin, B.B., Bidigare, R.R., Smith, R.C., 1993. In situ photosynthetic quantum yield. Correspondence to

hydrographic and optical variability within the Southern California Bight. Marine Ecology Progress Series 93, 25–37.

Sosik, H.M., 1996. Bio-optical modeling of primary production: Consequences of variability in quantum yield and specific absorption. Marine Ecology Progress Series 143, 225–228.

Sosik, H.M., Mitchell, B.G., 1991. Absorption, fluorescence, and quantum yield for growth in nitrogen-limited *Dunaliella tertiolecta*. Limnology and Oceanography 36, 910–921.

Sosik, H.M., Mitchell, B.G., 1994. Effects of temperature on growth, light absorption, and quantum yield in *Dunaliella tertiolecta* (Chlorophyceae). Journal of Phycology 30, 833–840.

Sosik, H.M., Mitchell, B.G., 1995. Light absorption by phytoplankton, photosynthetic pigments, and detritus in the California Current System. Deep-Sea Research I 42, 1717–1748.

Soto-Mardones, L.A., Parés-Sierra, A., García, J., Durazo, R., Hormazabal, S., 2004. Analysis of the mesoscale structure in the IMECOCAL region (off Baja California) from hydrographic, ADCP and altimetry data. Deep-Sea Research II, this issue [doi:10.1016/j.dsr2.2004.05.024].

Tomczak, M., Godfrey, J.S., 1994. Regional Oceanography: An Introduction. Pergamon Press, New York, 422pp.

Venrick, E.L., Hayward, T.L., 1984. Determining chlorophyll on the 1984 CalCOFI surveys. California Cooperative Oceanic Fisheries Investigations Reports 25, 74–79.

Yentsch, C.S., Menzel, D.W., 1963. A method for the determination of phytoplankton chlorophyll and phaeophytin by fluorescence. Deep-Sea Research 10, 221–231.